# Chiral Hydroxypropyl Cellulose and Nanocellulose Liquid Crystal Structural and Phase Behavior Elucidation and Their Photonic Elastomer Advanced Manufacturing – A Review

Jinlong Zhang,<sup>a,\*</sup> Cornelis F. De Hoop,<sup>b</sup> Qinglin Wu,<sup>b,\*</sup> and Ioan Negulescu <sup>c</sup>

In view of a need for high-performing materials, while also minimizing contributions to plastic pollution, especially ocean micro- or nano- plastic pollution, biodegradable hydroxypropyl cellulose (HPC) and nanocellulose (CNC) liquid crystal biopolymers have attracted attention as emerging fields. Their structures, phase behaviors, and advanced characterization techniques in terms of synchrotron X-ray and neutron small angle scattering of HPC solutions and CNC suspensions have been systemically studied. Diverse left- and right-hand chiral liquid crystal HPC and CNC photonic elastomer materials are further explored. To achieve their complex structure design and mass-scale manufacturing, soft matter photonic materials *via* advanced manufacturing techniques are critically considered in this review. The goal is to enable their applications in intelligent coating, photonic fiber, and intelligent packaging.

DOI: 10.15376/biores.19.4.Zhang3

Keywords: Liquid crystal; Hydroxypropyl cellulose; Nanocellulose; Synchrotron X-ray small angle scattering; Photonic elastomer; Additive manufacturing

Contact information: a: School for Engineering of Matter, Transport and Energy, Arizona State University, Tempe, AZ 85287, USA; b: School of Renewable Natural Resources, Louisiana State University Agricultural Center, Baton Rouge, LA 70803, USA; c: Department of Textiles, Apparel Design and Merchandising, Louisiana State University Agricultural Center, Baton Rouge, LA 70803, USA; \*Corresponding author: jzhan620@asu.edu and jinlongzhang914@gmail.com; QWu@agcenter.lsu.edu

#### INTRODUCTION

As plastic pollution issues have attracted significant attention recently, the development of cellulose liquid crystal materials that have potential to degrade is of significant interest (Frank *et al.* 2021; Erdal and Hakkarainen 2022; Bading *et al.* 2024). A liquid crystal has both crystal and liquid features. It displays a directional order like these of crystals, while retaining flowing similar to liquids. It can be divided into two main classes, thermotropic and lyotropic ones (Odian 2007). The cholesteryl derivatives, whose liquid crystalline phases are formed when the pure compound is heated, are named thermotropic, while those where the liquid crystalline phase forms when the molecules are mixed with a solvent are called lyotropic (Cowie and Arrighi 2007). Compared to the conventional synthetic liquid crystal materials, liquid crystal materials derived from cellulose have unique characteristics, such as (1) potential biodegradability and abundant resources, (2) both thermotropic and lyotropic liquid crystal properties, and (3) cholesteric or chiral nematic liquid crystal structure. The term chiral usually describes an object that is non-superposable in its mirror image (Solomons and Fryhle 2011). For instance, objects

that can exist in right-handed and left-handed forms are named chiral. A cholesteric or chiral nematic structure is formed by pseudo-layers of molecules aligned with a preferred direction, with the orientation of each layer rotated by a fixed angle around the cholesteric perpendicular axis (Ko et al. 2021), as depicted in Fig. 1D. Therefore, liquid crystal materials derived from cellulose and its derivatives have attracted attention, e.g., cellulose triacetate, nanocellulose (CNC), and hydroxypropyl cellulose (HPC). As a distinct state of matter, liquid crystals exhibit both optical birefringent characteristics of crystals and retain mechanical properties of liquids, as shown in Fig. 1A. The liquid crystal structures primarily include the nematic, smectic, and cholesteric ones (Fig. 1A). The unique texture structures of liquid crystals under the optical microscopy are shown in Fig. 1(B-D). Typical liquid crystal material consists of rigid mesogens and soft segments (Cowie and Arrighi 2007). By contrast, the rigid segments of anhydroglucose rings in cellulose work as liquid crystal mesogens, and the internal rotations of ether bonds between two anhydroglucose rings impart cellulose chain flexibility, so cellulose as a semi-rigid polymer, theoretically is able to form a liquid crystal structure. However, due to its low solubility in common solvents, it is hard to reach the critical concentrations in liquid crystal structure formation, so its lyotropic liquid crystal nature was initially thought not to be established.

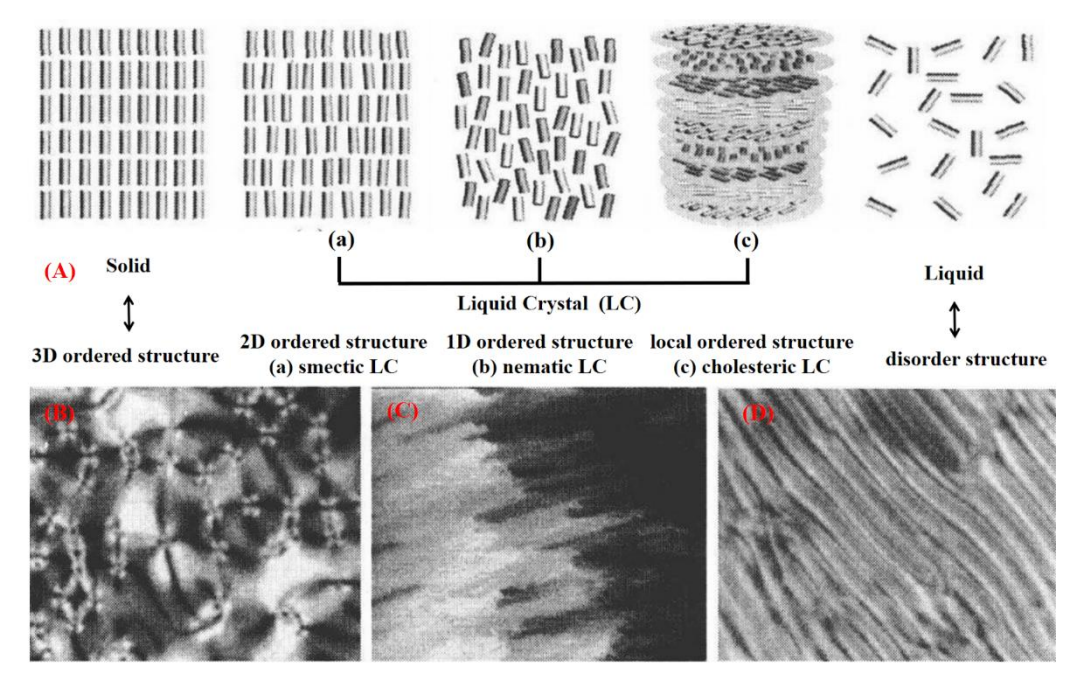


**Fig. 1.** Liquid Crystal (LC) Structure (A) [(a) smectic LC, (b) nematic LC, and (c) cholesteric LC] and Its Characteristic Texture Structures under Optical Microscopy [(B) nematic LC, (C) smectic LC, and (D) cholesteric or chiral nematic LC] (He 2020). Figure republished with permission from He (2020).

In 1959, the liquid crystal birefringent formation in aqueous gels of cellulose and chitin crystallites at a concentration more than 13 wt% was reported by Marchessault *et al.* (1959), but the helicoidal textures were not observed. In 1976, Prof. Gray at McGill University found the obvious iridescent color and birefringence property of HPC aqueous solution at concentrations within 20 to 50 wt% (Werbowyi and Gray 1976). As a derivative of cellulose, HPC is synthesized *via* the esterification reaction, in which some of the hydroxy groups in a linear cellulose backbone are hydroxypropylated. The substitution

reactions on the surface hydroxyl groups of cellulose destroy its original intra- and interhydrogen bonding interactions, thereby obviously increasing its solubility in water. Various cellulose derivatives (e.g., ethyl cellulose and cellulose triacetate) were then discovered to form the lyotropic liquid crystal structure in appropriate solvents. In addition to the type, size, and degree of substitution in substitution groups, the liquid crystal phase formation in these cellulose derivatives was found to be influenced by several factors, such as molecular weight and interaction with solvents. In 1992, Prof. Gray further reported the chiral liquid crystal texture structure of cellulose crystallites from optical microscopy, and the solid film from its casting suspensions displayed iridescent colors (Revol et al. 1992). In addition to cellulose crystallite, chitin crystallite also showed the nematic liquid crystal order and iridescent color. According to the circular dichroism spectroscopy, HPC aqueous solution in given concentrations formed a right-handed chiral nematic liquid crystal structure, while CNC and chitin nanocrystal aqueous solutions formed a left-handed chiral nematic liquid crystal structure in given concentrations. A counterclockwise twist denotes left-handed chirality, while a clockwise twist means right-handed chirality (Solomons and Fryhle 2011). Therefore, HPC and CNC as representative cellulose liquid crystal materials are discussed in this review in terms of their liquid crystal structures and phase behaviors in solutions or suspensions and when these effects are incorporated into flexible elastomer materials.

#### LIQUID CRYSTAL HPC SOLUTIONS AND CNC SUSPENSIONS

# **Basic Properties of Liquid Crystal HPC and CNC**

HPC is a derivative of cellulose that was originally developed by the US Hercules Chemical Company at Wilmington, Delaware. It is usually synthesized by the reaction of hydroxyl groups of cellulose with propylene oxide by ring opening cross etherification in alkali conditions, and its degree of substitution of hydroxypropyl groups is typically from 2.5 to 4. As an aspect of its unique behavior, the water-soluble HPC is only soluble below its critical solution temperature, named as low critical solution temperature (LCST), at approximately 42 °C. HPC spontaneously organizes into a right-handed chiral nematic liquid crystal arrangement in its aqueous solutions. Such solutions exhibit iridescent colors when its concentration of aqueous solutions reaches above 40 wt% (Yi et al. 2019; Singh et al. 2022; Chen et al. 2023). Its cholesteric liquid crystal phase is also tunable to reflect wavelengths across the entire visible spectrum. For example, as the concentrations of HPC aqueous solutions are from 50 to 70 wt%, the structural colors from red to blue can be observed by its self-assembly into a cholesteric structure (Zhang et al. 2021; Bai et al. 2021). In addition to its solubility in water, more hydrophobic 2-hydroxypropyl side chains combined with the hydrophilic cellulose backbone gives its solubility in a range of organic solvents (Godinho et al. 2017). Most importantly, if the solvents enable it to be polymerized under given conditions, the chiral nematic liquid crystal can be locked in the cross-linked polymer networks, thereby producing HPC composite materials with the chiral nematic liquid crystal structures (Zhang et al. 2022). Interestingly, its composites display unique optical properties (Werbowyj and Gray 1984; Chan et al. 2019). For instance, HPC composite hydrogels were found to display color-responsive properties under external stimuli (Shi et al. 2023).

In addition to its self-assembly into a cholesteric liquid crystal structure, HPC aqueous solutions has a temperature-responsive property with a low critical solution

temperature (LCST) at about 42 °C, like poly(N-isopropylacrylamide) [PNIPAM], as its solubility decreases above its low critical solution temperature, resulting in phase transition and causing light scattering (Zhang et al. 2017; Shi et al. 2023). Therefore, when heated above its LCST, HPC aqueous solutions undergo a volume-phase transition and then become turbid because the entropically driven release of water molecules leads to the formation of HPC coils and these subsequently collapse into globules (Gao et al. 2001; Weißenborn and Braunschweig 2019; Vogler-Neuling et al. 2023). This unique property of HPC makes it an ideal thermo-responsive material. The water-cast HPC films also display the thermotropic liquid crystalline optical property when heated (Winnik et al. 1987). Although HPC liquid crystal and its temperature responsive optical property have been discovered several years ago, their nematic liquid crystal photonic materials has attracted attention just in the most recent years, which can be attributed to the increasingly demanding for sustainable material around the world (Zhang et al. 2023). Therefore, the study in terms of HPC nematic liquid crystal and its optical property is still in its infancy and demanding further investigations in terms of phase transitions, temperature on its phase transitions, and phase separation behaviors.

Whereas the HPC with right-handed chiral nematic liquid crystal structure, CNC can self-assemble into nematic liquid crystal structure with a left-handed chirality. CNC is a rod-like nanomaterial with unique properties, such as large aspect ratios, high modulus, abundant surface groups, and sustainability. Therefore, CNC has attracted attention initially for reinforced nanocomposites. CNC is primarily prepared from TEMPOmediated oxidation, sulfuric acid hydrolysis, and ammonium persulfate oxidation methods. CNC produced via sulfuric acid hydrolysis as the conventional method has been widely studied. The produced negatively charged sulfate groups on the surface of CNC promotes its uniform dispersion in water via electrostatic repulsion when sulfuric acid works as the hydrolyzing agent. Thus, CNC aqueous solutions at a given concentration have characteristic texture structure under optical microscopy and nematic liquid crystal properties. The electrostatically stable CNC liquid crystal structures are also dependent on other parameters, such as sizes, surface charges, and suspension concentrations (Hubbe et al. 2017). Although Marchessault discovered the liquid crystal property of cellulose crystallites in 1959 (Marchessault et al. 1959), its chiral nematic liquid crystal structure study started just a few years ago. Therefore, the next section is about the structure and phase behavior of liquid crystal HPC and CNC.

#### Hierarchical Structure and Phase Behavior of HPC and CNC

Multi-level structures of HPC and CNC

Like the hierarchical structures of protein and silk fibroin, HPC and CNC are composed of multi-level structures, namely, primary, secondary, and tertiary structures (Solomons and Fryhle 2011). The primary structure is referred to as the sequence of small molecular residues making up the polymers, e.g., different amino acids in proteins, while the secondary structure is the spatial arrangement of a chain, e.g., the random coil and helical conformations of protein (Atkins and Paula 2010). The repeated unit of both CNC and HPC as the primary structure is composed of two anhydroglucose rings linked together through an oxygen atom via covalent bonding to C1 of one glucose ring and C4 of the adjoining ring through a  $\beta$ -1,4 glucosidic bond, while a linear cellulose backbone is further etherified with hydroxypropyl groups with a typical degree of substitution from 2.5 to 4 in HPC. The chemical structure of HPC and CNC repeated unit is primarily determined via proton nuclear magnetic resonance (NMR) spectroscopy, while CNC chemical structure

was primarily confirmed by solid-state NMR spectroscopy, due to its low solubility in deuterated solvents (Zhang et al. 2017). The HPC and CNC chain conformation (flexibility and rigidity) and its size (molecular weight and its dispersion) as the secondary structure are composed of multiple repeated units of anhydrogluose rings. Their weight average molecular weight, number average molecular weight, and poly-dispersion are primarily measured via the gel permeation chromatography, light scattering, and asymmetric field flow fractionation (Guan et al. 2012). For the tertiary structure of HPC and CNC, the aggregates of multiple chains through inter-chain hydrogen bonding interactions form the chiral liquid crystal structures. Taking the hierarchically helical structure of CNC as an example, it is composed of superimposing planar layers, and within each layer, rod-like CNC are arranged in parallel-alignment under a given twisting angle (Zhang et al. 2023). The chirality, pitch, rod-like mesogen arrangement, and orientation of HPC and CNC cholesteric liquid crystal phase are usually measured via the circular dichroism spectroscopy, wide-angle X-ray diffraction, and polarized optical microscopy.

As is well known, a polymer has no gas state, and research in terms of HPC and CNC chain conformation and aggregation state usually starts from its aqueous solutions. As the concentrations of HPC aqueous solutions or CNC aqueous suspensions increase, the numbers of HPC or CNC chains increase; then they interact and interpenetrate with each other to form chain entanglements or aggregations. Therefore, the research in terms of liquid crystal aggregation status from HPC single chain or CNC rod-like crystalline into chiral nematic liquid structure is parallel to the process from diluted HPC solutions or CNC suspensions to its concentrated solutions. However, CNC is not water-soluble and exists in aqueous suspensions, while HPC is water soluble and forms homogeneous aqueous solutions, so it follows the rule of Mark-Houwink relationship. Thus, HPC as a representative is further explored for its conformation and stiffness. In the dilute solution (less than 40%), the conformation and stiffness of HPC chain are usually determined by viscosity measurements using the Mark-Houwink relationship 1 (Hiemenz and Lodge 2007).

$$[\eta] = KM^{\alpha} \tag{1}$$

where K and  $\alpha$  are constants for a given polymer-solvent system, and M and  $[\eta]$  are the molar mass and limiting viscosity. The value of the Mark-Houwink exponent  $\alpha$  ranges from 0.5 as Gaussian coils to 1.8 as rigid rods in solutions (Rubinstein and Colby 2003). According to the literature,  $\alpha$  was found to be 0.90 for the diluted HPC aqueous solution (Werbowyj and Gray 1984). Therefore, the HPC chain is neither rigid nor rod-like in dilute solutions, and dilute HPC aqueous solutions behave intermediate between the rod-like molecules and random coils. In addition, the HPC chain has a straight helical conformation, which can be attributed to its intra- molecular hydrogen bonding interactions, which have been confirmed via X-ray diffraction. Its HPC chain conformation can be ideally described by the semi-flexible or worm-like chain model (Rubinstein and Colby 2003; Hiemenz and Lodge 2007), and thus its properties lie intermediate between random coils and rigid rods. According to the worm-like chain model, the Kuhn segment length and chain flexibility or rigidity of HPC chains as key parameters govern its liquid crystal cholesteric structure formation. The flexibility of HPC chain is usually determined by its Kuhn segment length according to the formula 2 (Rubinstein and Colby 2003),

$$l' = \frac{\langle r_0^2 \rangle}{nl} \tag{2}$$

where n and l are the number of polymer chain and its length, and  $< r_0^2 >$  is the mean square unperturbed end-to-end distance of a polymer chain, respectively.

By contrast, HPC chains form a chiral nematic liquid crystal structure with a wellordered planar texture arrangement in its concentrated aqueous solutions above 40% (Casay et al. 1995). The characteristic fingerprint-like pattern of HPC cholesteric liquid crystal solutions can be observed by means of polarized optical microscopy. However, the HPC cholesteric liquid crystal structure formation has requirements, namely, (1) the straight helical conformation as the first necessary condition, (2) the lack of flexibility in cellulose backbone contributing for an ordered phase formation, and (3) the cholesteric liquid crystal phase formation driven from chirality of anydroglucose repeat units. The liquid crystal order in HPC is primarily evaluated by its helicoidal supramolecular arrangement. It is composed of superimposing planar layers, and within each layer, the stiff HPC chains are arranged in linear and parallel alignment under a given twisting angle. The average intermolecular distance of the cholesteric liquid crystal phase can be confirmed by X-ray diffraction (Werbowyj and Gray 1984). The average intermolecular distance is less dependent on its concentration, as the side substituent propyl groups in the HPC molecule are too short to be folded. Like most polymer lyotropic cholesteric liquid crystal solutions, the pitch as another important parameter of HPC cholesteric liquid crystal structure is correlated with its concentration, degree of substitution, and molecular weight (Vshivkov and Rusinova 2007). As HPC and CNC liquid crystal structure impacts its phase behavior, the next section is about the phase behavior of liquid crystal HPC and CNC.

### Phase behavior of liquid crystal HPC and CNC

The HPC phase behavior and its transition can be described by phase diagram, as shown in Fig. 2 (Werbowyj and Gray 1980). As HPC is a temperature-responsive polymer with LCST value, its cholesteric liquid crystal solution is temperature-responsive. Thus, both concentration and temperature parameters govern its liquid crystal phase behavior. Therefore, the research in phase transition behavior of HPC aqueous solution follows these clues. Namely, the HPC phase behavior's dependency on its concentration is established at the constant temperature, and its phase behavior that relies on temperature is then established at the constant concentration.

In general, HPC solutions involve four different phases, isotropic, biphasic, anisotropic, and gel regions. The general feature of its phase diagram was reported by Prof. Gray at McGill University. At constant temperature (20 °C) lower than its LCST value, the isotropic phase is stable up to critical concentration at 38 wt%, and the biphasic region occurs between 39 and 47 wt% of HPC concentration. The biphasic phase means a polymer-rich phase, and a more dilute isotropic phase exists in equilibrium and displays a high birefringent and brilliant color viewed between crossed polar optical filters. As the concentration further increases, a 100% anisotropic phase is established at 49 wt% HPC critical concentration.

A slight difference in terms of critical concentration of anisotropic phase formation happens for different molecular weights or degrees of substituent in the side chain of HPC. Cholesteric colors then appear in the pure anisotropic phase between 51 and 70 wt% concentration of HPC, while as the critical concentration increases, the colors change from red to violet, which can be attributed to the decrease in the cholesteric helix pitch (Vshivkov and Rusinova 2007).

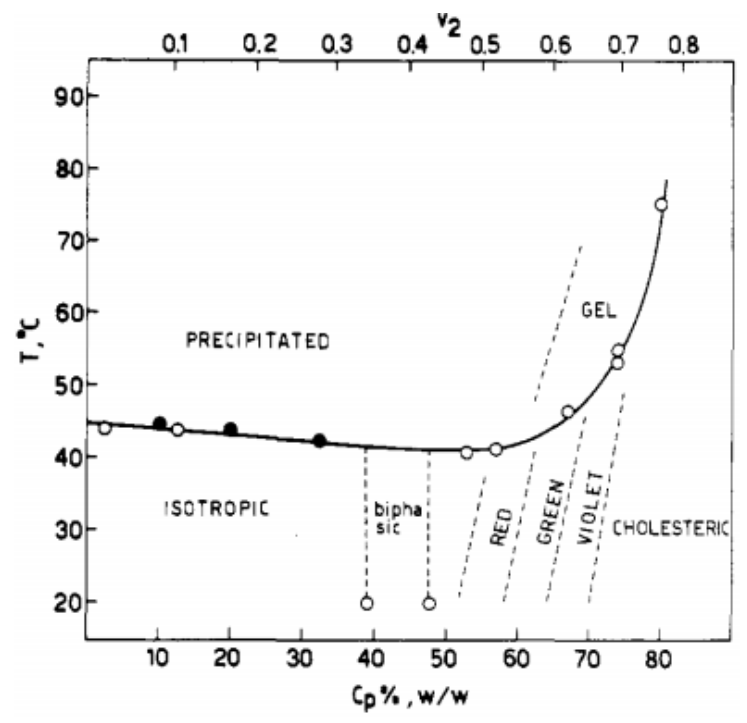


**Fig. 2.** Phase diagram of HPC aqueous solutions (Werbowyj and Gray 1980). Figure reprinted with permission from Werbowyj and Gray (1980), *Macromolecules* 13, 69-73, Copyright 1980, American Chemical Society.

In addition to the HPC concentration, temperature is another factor that governs phase transition of HPC cholesteric liquid crystal solutions. The diluted HPC solutions with the concentration lower than 40 wt% are isotropic at the ambient temperature, while they are cloudy upon heating. A concentrated white phase as roughly spherical particles having diameters near to 1 µm is physically separated from this clear and fluid solutions upon heating at high temperature in a sufficiently longer time, such as a few days. This phase separation is analogous to the process of heating other blends of water with non-polymeric and polymeric solutes, as this physically separated white phase has no birefringence observed under the optical microscopy. Upon further heating, this concentration phase coagulates and comes out as a precipitated phase, which is very viscous but exhibits definite fluidity (Fortin and Charlet 1989). By contrast, as HPC concentrations are at more than 40 wt%, the cholesteric colors in the concentrated solutions can be observed resulting from the HPC anisotropic phase. The further increase in the concentration of HPC solutions shifts colors toward the violet end. As HPC colors are sensitive to temperature, the concentrated HPC solutions turns into an increasingly intense white upon heating over a wide temperature range. Most importantly, the cholesteric colors are reversible, as they return instantly upon cooling (Werbowyj and Gray 1980). As the further increase of concentrations, the appearance of the precipitate changes from a white suspension of particles to a semitransparent gel upon heating (Conio et al. 1983; Guido 1995).

Compared to HPC, the CNC phase diagram is relatively simple, as CNC phase behavior is primarily dependent on its concentration. The cholesteric CNC liquid crystal phase formation also occurs above a critical concentration. In addition to its concentration, its phase behavior also depends on the solvent properties. However, most studies in terms of CNC cholesteric liquid crystals have been restricted to aqueous CNC solutions until now, while a clear relationship can be confirmed. Namely, as the concentrations of solvents

increases, a reduction in the chiral nematic pitch can be observed (Pan *et al.* 2010; Cheung *et al.* 2013; Bruckner *et al.* 2016). For CNC aqueous suspensions, three phases are normally formed in a range of concentrations, namely, isotropic, biphasic, and cholesteric liquid crystal phase. At low CNC concentrations, the isotopic region occurs, in which the rod-like CNC is randomly orientated. The CNC suspensions form biphasic phases, namely, chiral nematic liquid crystal and isotropic phases at the critical concentration between 3 and 10 wt%. As the transition from isotropic to biphasic phase, the liquid crystal phase is first formed from the larger particles, and the rest of small particles are still in the isotropic phase. (Browne *et al.* 2022). As the concentrations of CNC suspensions is reached at about 12 wt%, CNC particle orients and transforms into a chiral nematic phase as a highly ordered twisted structure.

# Characterization of Liquid Crystal HPC Solutions and CNC Suspensions

Studies of structure and phase transition of chiral nematic liquid crystals of HPC solutions and CNC suspensions have made a large progress. However, some discrepancies and unexplored areas still need to be further investigated, *e.g.*, the exact numbers of phase regions in HPC and CNC phase diagrams, phase behaviors at high temperature of HPC solutions, and nanoscale orientation of individual CNC nanocrystals. Therefore, all of these questions are highly dependent on the advanced characterization tools, especially synchrotron X-ray and neutron small angle scattering equipment. Therefore, this section primarily focuses on the advanced characterization of liquid crystal HPC solutions and CNC suspensions.

## Polarized optical microscopy and circular dichroism spectroscopy

Polarized optical microscopy is a straightforward method for the liquid crystal structure characterization by recording the optical texture image resulting from the defeat and orientation of director in the sample. The structure of HPC and CNC liquid crystalline phases shows a characteristic fingerprint-like pattern that results from the cholesteric structure observed from the right angles to the cholesteric axis under the polarized optical microscopy (Sun 2004). Half of the pitch in the nematic HPC or CNC liquid crystal structure corresponds to the spacing of alternative dark and light lines in their supermolecular helicoidal arrangement. In addition, circular dichroism (CD) spectroscopy is an important tool to identify molecular chirality (Solomons and Fryhle 2011). Thus, the chiral nematic orientation of HPC liquid crystal solutions and CNC liquid crystal suspensions is primarily confirmed *via* the CD spectroscopy. As the CNC liquid crystal helical twist displays a left-handed nature, the chiral nematic orientation of CNC primarily produces a negative signal when subjected to the CD spectroscopy. In contrast, the chiral nematic orientation of HPC usually yields a positive signal when subjected to CD spectroscopy, as the HPC liquid crystal helical twist exhibits a right-handed nature (Sun 2004).

#### Rheology and (rheo-) small angle X-ray and neutron scattering

Rheology is an ideal tool to study the phase behavior of liquid crystal HPC solutions and CNC suspensions, as the rheology response of liquid crystal polymers during shear flow reflects a strong relationship between the rheological property and phase state. The phase transition can be observed by viscosity change in the isotropic and nematic phases due to the competition in shear and packing order of molecules in solution supported by polarized optical microscopy observation as the solutions reach a critical concentration (Hubbe *et al.* 2017). The rheological property of liquid crystal solutions under the flow is

of interest for practical applications in extrusion-based 3D printing and wet-spinning of fibers (Kulichikhin *et al.* 2011). However, the liquid crystal solution structure variations are not easily observed in rheological measurements directly. Small angle X-ray scattering (SAXS), is a powerful tool to examine the structure evolutions of liquid crystal solutions at the length scale of nanometers. For low q-values, the measurement of scattering at small angles reaches particle interactions, while the investigation of scattering at relatively large angles (less than 6 degree) reaches the particle surface at high q-values (Roe 2000). Therefore, scattering methods combined with rheology accessories are unique tools for detecting structure and phase behaviors of liquid crystalline HPC solutions and CNC suspensions under flow. Therefore, the sizes and spacing features of liquid crystal HPC solutions or CNC suspensions from the Rheo-SAXS measurement can translate into the degree of order (Kádár *et al.* 2021). A schematic Rheo-SAXS instrument is shown in Fig. 3 (Pignon *et al.* 2021).

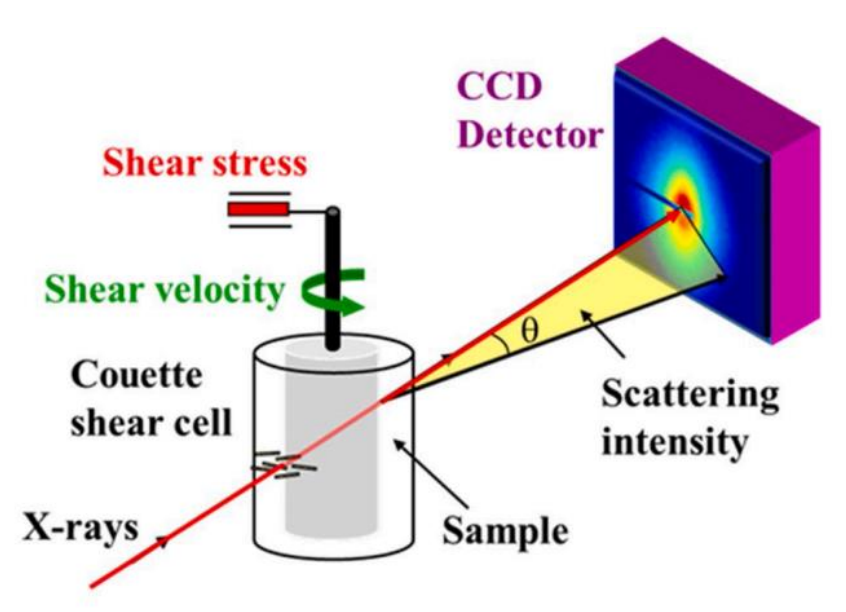


**Fig. 3.** Schematic Rheo-SAXS Equipment for Investigation of Liquid Crystal HPC Solutions and CNC Suspensions (Pignon *et al.* 2021). Reprinted with permission from Elsevier Publishing Co.

In addition to SAXS, the degree of orientation in longer-range arrangements (ordered textures) can be determined by the wide-angle X-ray scattering (WAXS). Thus, by combining scattering and rheological analysis, namely, Rheo-SAXS and Rheo-WAXS, the size, structure, phase behavior, and orientation of HPC solutions or CNC suspension under the shear deformation can be determined. For instance, the microstructure transition of CNC liquid crystal dispersion and shear induced its alignment were confirmed by the Rheo-SAXS instrument. However, the scattering contrast of liquid crystal HPC solutions or CNC suspensions is weak, so it is not easy to directly observe the alignment or anisotropy generated from HPC chains or CNC rods under the shear deformation. Rheo-small angle neutron scattering (Rheo-SANS) provides an efficient scattering contrast by means of deuteration to evaluate the degree of anisotropy or alignment in the microstructure change of HPC solutions or CNC suspensions under the shearing deformation. Therefore, the microstructure order (molecular alignment, mesogenic orientation, and orientation of lamellar stacking at the longer-range scale) and rheology

behavior of liquid crystal HPC solutions or CNC suspensions can be understood by Rheo-SANS (Haywood *et al.* 2017).

#### LIQUID CRYSTAL HPC AND CNC PHOTONIC ELASTOMER

Although the chiral nematic CNC or HPC liquid crystals can be well-preserved in their self-assembled dry films, their susceptibility to redissolution in water and brittleness are challenging issues. An elastomer has unique merits in terms of robust mechanical and flexible properties, which makes it possible to prepare CNC or HPC liquid crystal films with enhanced water resistance and flexibility property via different polymerization approaches. Therefore, hydrogel, ionic gel, conventional cross-linked elastomer, and chemically recycled cross-linked elastomer with a dynamically covalent cross-linking are ideal soft matters to tailor HPC or CNC film property discussed in this section.

# Liquid Crystal HPC and CNC Photonic Hydrogels and Ionic Gels

A tough hydrogel material with double network cross-linked structure was discovered by Prof. Gong from Hokkaido University, Japan in 2003 (Gong et al. 2003). This approach was further extended toward diversely intelligent hydrogels via the physical and chemical cross-linking strategy by Prof. Suo from Harvard University, USA in 2012 (Sun et al. 2012). To design tough hydrogel materials, nanomaterial was further explored as reinforced fillers and physical cross-linking points for the development of highperformance hydrogel materials since that time. Especially, CNC-reinforced hydrogel materials have attracted attention due to their high modulus, hydrophilic property, and abundant surface groups. Due to its unique merits in terms of chiral optical and photonic color responsive property, CNC has attracted interest in design of photonic hydrogel materials recently. Inspired by chamelelons, the structural colour variation of its skin is attributed to the locked helical variation of photonic crystals inside of cells. Photonic crystals are usually generated by self-assembly of colloidal particles with a periodic lattice, e.g., silica oxide photonic crystal particles (Wang et al. 2021). The mechanically induced color-responsive CNC doped photonic hydrogel materials was first reported from Prof. MacLachlan at University of British Columbia. Therefore, physically cross-linked photonic hydrogel materials were then developed, but the durability and stability of its structural colors were big issues. Therefore, the chemically cross-linked photonic hydrogel materials were further explored by in situ polymerizing monomers in the presence of selfassembled CNC (Peng et al. 2020). Namely, chiral cellulose particles doped into monomer and cross-linker solutions forms the cross-linked network structural hydrogels via the stepgrowth and chain growth polymerization, and the resulted photonic hydrogels exhibits unique color responsive properties under the external mechanical stimulus. As the CNC or HPC chiral helical structure is sensitive to external environmental conditions, such as ionic strength or pH, the challenging issues in successful preparation of chemically cross-linked photonic hydrogel is how to find the appropriate polymerization conditions of hydrogel precursors under the prerequisite of retaining the established CNC or HPC chiral helical structure. Thus, CNC-reinforced polyacrylamide photonic hydrogels were explored for the design of robust photonic hydrogels as the increased hydrogen bonds of acrylamide monomers and CNC or HPC promoted the self-organization of chiral CNC or HPC liquid crystals and resulted in the generation of brilliant photonic colors. To address the sensitivity issues of CNC or HPC liquid crystal structure, an alternative method for photonic hydrogel preparation was also reported. Namely, CNC liquid crystal film was soaked into the initiator, monomer, and cross-linker solutions; then CNC photonic hydrogels were produced by thermal polymerization, and the resulting CNC composite hydrogels provided stimuli-responsive property with reversible structural colors and fast response upon the mechanical stretching (Babaei-Ghazvini and Acharya 2023).

In addition to the single responsive photonic hydrogels, the development of dual responsive photonic hydrogels has also attracted significant attention. As mentioned in the previous section, PNIPAM is a temperature-responsive polymer with an LCST value, and the transmittance and swelling ratio of the resulting PNIPAM hydrogel materials is dependent on temperature. Therefore, the swelling and shrinking performance of PNIPAM hydrogel materials could transform a thermal stimulus into a photonic color change (Wang et al. 2021). For instance, the pressure and temperature-responsive photonic hydrogels based on stearyl acrylate, NIPAM, and N,N'-methylene bisacrylamide (MBA) was reported, and the PNIPAM chains imparted photonic hydrogels with a temperature responsive trait. In addition, hydrophobic microdomains of stearyl acrylate segment endowed the photonic hydrogels with enhanced pressure and temperature dynamic structure colors and enhanced the physical cross-linking points and interfacial hydrogen bonds, providing supports for the reliability and reversibility of the resulted photonic hydrogels (Li et al. 2022, 2023). However, temperature-responsive PNIPAN as a functional component is required to achieve the dual responsive property in CNC photonic hydrogels. Therefore, there is a high demand to develop cellulose liquid crystal photonic hydrogels with intrinsic multi-responsiveness. HPC liquid crystal solutions, which have both mechanical and temperature dual responsive properties, have become an emerging candidate for photonic hydrogel design with intrinsic multi-responsive structural color property. For instance, the HPC, 2-acrylamido-2-methylpropane sulfonic acid monomer, and 2-hydroxyl-4'-(2-hydroxyethoxy)-2-methylpiophenone cross-linker, (Irgacure 2959) as a photo-initiator were prepared for cross-linked hydrogels, and the resulting photonic hydrogels displayed both temperature and mechanical responsive structural colors, as shown in Fig. 4 (Shi et al. 2023).

Compared to conventional hydrogel materials, ionic conductive gels with robust mechanical property, reliable electrical conductivity, and good biocompatibility have attracted interest. As a new type of ionic liquid, deep eutectic solvent (DES) is composed of a hydrogen bond acceptor and hydrogen bond donor in the form that exhibits complexation (Isik *et al.* 2016). Interestingly, the polymerizable DES (PDES) ionic gels composed of the ionic polymer chain backbone and counter ions self-associated by hydrogen bonding are intrinsically ionic conductive, flexible, and stable, as shown in Fig. 5 (Fei *et al.* 2023). For instance, mechanochromic chiral nematic CNC-PDES ionic gels prepared by the infiltrating PDES into a self-assembled CNC film followed by light polymerization exhibited the ionic conductivity and outstanding sensing performance in terms of electrical and optical dual signal responsiveness (Li *et al.* 2023). Similarly, the PDES ionic gels with physically and chemically dual cross-linking networks *via in situ* polymerization of PDES was applied in the wearable sensors (Lu *et al.* 2022).

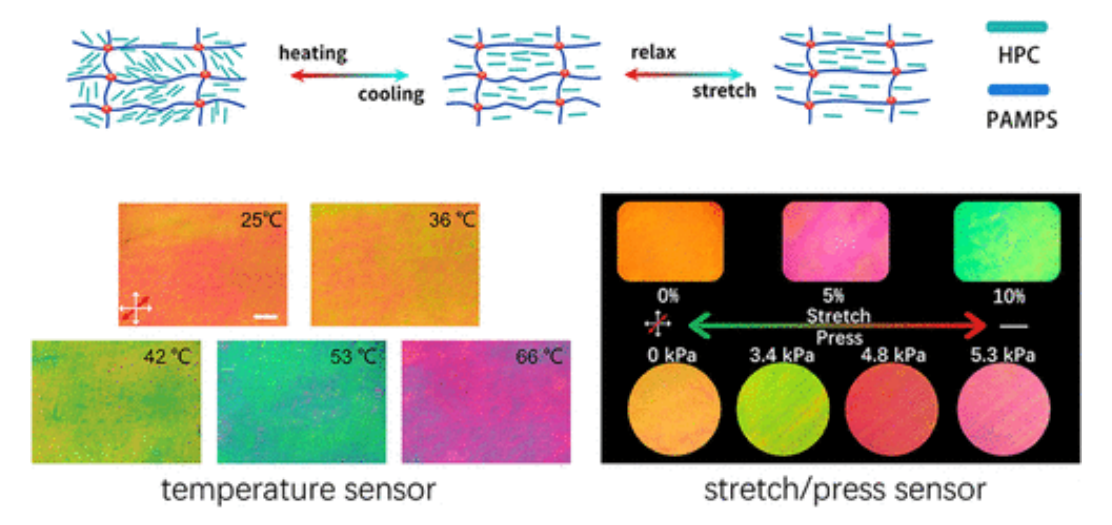


**Fig. 4.** HPC hydrogel temperature and mechanical responsive color sensor (Shi *et al.* 2023). Reprinted with permission from Shi *et al.* (2023), *ACS Applied Nanomaterials*, 6, 11524-11530. Copyright 2023, American Chemical Society.

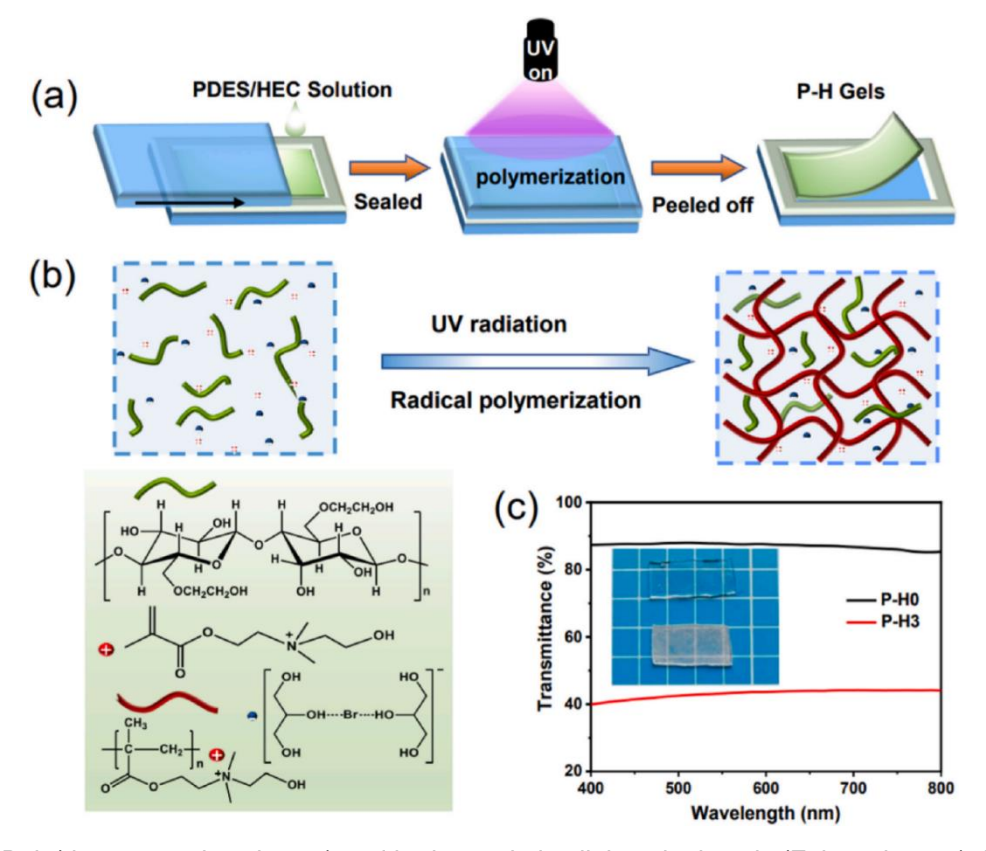


**Fig. 5.** Poly(deep eutectic solvents) and hydroxyethyl cellulose ionic gels (Fei *et al.* 2023). Figure republished with permission from Elsevier Publishing Co.

For the purpose of recycling, a recyclable ionic gel *via* the dynamic covalent crossling of polyvinyl alcohol and dialdehyde carboxymethyl cellulose in the deep eutectic solvents was further explored (Cui *et al.* 2022). However, all these cases have no mentions in terms of liquid crystal photonic properties. Therefore, the study of HPC or CNC doped

PDES elastomer photonic materials with both ionic conductivity and recycling property is an emerging field.

# **Conventional and Dynamic Covalent Cross-linked Photonic Elastomer**

As hydrogels or ionic gels have issues in terms of reduction in flexibility resulting from solvent loss in long-term utilization, there is a great need for stable and reliable photonic elastomers with excellent comprehensive properties. Polyurethane (PU), polydimethylsiloxane (PDMS), and polyacrylate as conventional elastomers have been explored for the design of photonic elastomer materials. Polyacrylate elastomers are relatively cheap and easily synthesized *via* free-radical polymerization, so they have potential in structural color coating applications. For the photonic polyacrylate elastomers, one design approach is to prepare the CNC liquid crystal photonic film *via* evaporation induced self-assembly.

The next step is impregnation into the monomer, initiator, and/or cross-linker solutions to synthesize the photonic elastomers via the light- and thermal polymerization. For instance, the photonic polyacrylate elastomers were prepared by infiltrating ethyl acrylate and 2-hydroxyethyl acrylate precursors into self-assembled CNC followed by polymerization (Chen and Hong 2020). Similarly, a piece of the CNC liquid crystal film was soaked in a solution of azobisisobutyronitrile to swell the film, followed by the addition of monomer solutions involving methyl methacrylate, methyl acrylate, 2-(3-(6-methyl-4-oxo-1,4-dihydropyrimidin-2-yl) ureido) ethyl methacrylate, and MBA. The robust and reversible mechanochromism of photonic polyacrylate elastomers *via* the conventional free radical polymerization was achieved (Boott *et al.* 2020; Boott *et al.* 2021).

The stretching pretreatment of CNC liquid crystal films before polymerization can further enhance the structural colors. For instance, CNC and polyacrylate elastomer composite materials were prepared *via* pre-stretching to get the alignment CNC liquid crystal in the elastomer matrix, thereby enhancing the brilliant structural colors (Kose *et al.* 2019). In addition to thermal initiation polymerization, a photoinitiated polymerization method to prepare stretchable chiral nematic CNC elastomer composites was also reported (Boott *et al.* 2023).

Another approach for synthetic CNC photonic elastomer is to directly mix CNC liquid crystals, monomers, initiators, and/or crosslinkers and then subject the mixture to polymerization under the thermal and light initiation. For instance, (ethylene glycol) diacrylate (EGDA) or 2-hydroxyethyl acrylate (HEA) and Irgacure 2959 were added to the CNC suspensions to obtain the uncross-linked CNC/EGDA or CNC/HEA film *via* the solvent evaporation followed by irradiating with an ultraviolet lamp to produce cross-linking polyacrylate elastomers (Qu *et al.* 2019; Momen *et al.* 2021; Boott *et al.* 2021; Kose *et al.* 2019).

In addition to the chain growth polymerization, the step-growth polymerization has also been explored for the synthetic CNC photonic elastomers. For example, CNC photonic film is prepared first and then impregnated in the prepolymer solution composed of 1,12-dodecanediol and citric acid, followed by thermal polymerization to produce the photonic elastomer materials (Espinha *et al.* 2016). In addition to the polyacrylate elastomer, the excellent biocompatibility, high flexibility, long flex life, and superior chemical stability of PDMS enable its applications in flexible and mechanochromatic skins. For instance, carbon nanotube (CNT) doped HPC liquid crystal was prepared. Crystal formation was attributed to HPC's amphiliphic property as a surfactant to stabilize CNT particles and its

CNT/HPC hybrid was further locked in PDMS matrix after thermal curing to obtain the CNT/HPC/PDMS photonic elastomer for flexible skins. As the temperature was increased from 0 to 40 °C, the colors of electronic skins showed a red shift due to the intrinsic thermal response property and thermally induced pitch variation. In addition to the temperature induced color change, as the hybrid PDMS elastomer exposed to pressure and tension stimuli, the electronic skins have a range of color variations (Zhang *et al.* 2020).

PU composed of hard segments and soft segments via the condensation polymers has also been widely explored in photonic elastomers. For instance, PU/CNC elastomer photonic film was prepared and displayed reversible optical tunability. In addition, great efforts have been made to prepare flexible and reversible structural color CNC/PU elastomer films via the layered pseudonematic and chiral nematic order switching (Zhang et al. 2020). In compared to the hydrophobic PU elastomer materials, waterborne PU elastomer has attracted interest for the design of CNC/WPU photonic elastomer, as WPU has a good miscible with water-soluble CNC liquid crystal suspensions, and the resulting WPU photonic elastomers exhibited dynamic photonic property, responding rapidly to external stimuli (Qu et al. 2019; Sui et al. 2020). As the photonic elastomer subjected to the repeated mechanical deformation lost photonic property and produce large amount of elastomer waste, the development of recyclable and self-healing photonic elastomer vitrimer via the dynamic covalent cross-linked structure has attracted attention. A flexible photonic elastomer with self-healing ability was prepared by combining WPU containing dynamic covalent disulfide bonds with CNC, and the elastomer film exhibited an amazing self-healing efficiency at room temperature (Xue et al. 2023). CNC doped hexanediamine cross-linked poly(butyl acrylate-co-2-(methacryloyloxy)-ethylacetoacetate) elastomer was found to be iridescent and birefringent (Vollick et al. 2017), and elastomer materials crosslinked by the dynamic covalent bonds also have a potential recycling property. However, the design of chemically recyclable photonic elastomer vitrimer is still less reported currently.

# ADVANCED MANUFACTURING OF HPC AND CNC SOFT MATTER PHOTONIC MATERIALS

The goals of mechanical flexibility or water solubility can be addressed by the hydrogels or elastomers locked CNC or HPC liquid crystal photonic materials. However, most of CNC or HPC liquid crystal photonic elastomer materials that are prepared *via* solution casting exhibit angle-dependent structural color due to the rapid shear exposure during the solution casting process. There is a high demand for manufacturing of soft matter photonic materials with angle-independent structure colors. The single/twin screw extrusion, injection molding, two-roll milling, and extrusion-based 3D printing or electro-/wet-spinning methods make it possible to control the shear exposure time of HPC or CNC liquid crystal photonic elastomer materials during advanced manufacturing process and therefore provide more opportunity to develop a uniformly aligned configuration of photonic elastomer materials with angle-independent structural colors (George *et al.* 2023; McCrum *et al.* 1997). How to produce HPC or CNC soft matter photonic materials in mass scale is also a tough question currently.

# **Conventional Manufacturing HPC or CNC Photonic Materials**

Ocean micro- or nano -plastics have attracted significant attention currently, as these plastic particles can't be degraded, and most of these plastic particles contain color pigments. Therefore, the development of environmentally friendly and biodegradable HPC or CNC pigments as an alternative to chemical pigments is a novel direction. For instance, the CNC photonic film was manufactured in mass scale via the roll-to roll coating technique, and the CNC coated photonic films displayed robust mechanical and solventresistant property after further thermal treatment (Droguet et al. 2022). This work provides a new idea using HPC or CNC pigments to manufacture color and solvent-resistant papers or fabrics in mass scale. In addition to roll-to-roll coating, spray coating is also frequently used in industry. There is also a need for spray coating polyacrylate and HPC or CNC hybrid materials on different substrates for decoration purposes (Wang et al. 2018; Ayrilmis 2020). The HPC-PDMS or PU elastomer composite coating via the spray or spinning coating probably responses to different environmental signals, so it could serve as a potential colorimetric sensor or intelligent packaging material. As HPC or CNC photonic colors can be well preserved after breaking them into small particles, the development of photonic HPC or CNC pigments reinforced plastic composites with vivid structure colors is promising manufactured in mass scale via the screw extruder, injection molding, hot-press, and thermoforming. The resulting color plastic materials have potential as alternatives of chemical dyes or pigments tailored high density polyethylene castor oil bottles or polyethylene terephthalate beverage bottles (Dong et al. 2023). However, the thermal stability of CNC in the melting extrusion is still a barrier in large-scale manufacturing.

# 3D Printing HPC or CNC Photonic Materials

3D printing makes it possible to design internal structures of printed elastomer photonic materials and to address issues in terms of angle dependent structural colors (Xie et al. 2023). As an extrusion-based 3D printing technique, direct ink writing (DIW) 3D printing is an ideal strategy to manufacture photonic elastomer materials with angle-independent structure colors. However, DIW 3D printing has special viscosity requirements to make sure that the printing inks extrude through the nozzle easily during the printing and the printed object also forms a self-standing structure on the arbitrary substrate after extrusion. Therefore, CNC and HPC work as both rheological modifiers and liquid crystal components for design of photonic elastomer materials (Ebers and Laborie 2020). For instance, HPC-gelation-poly (acrylamide-co-acrylic acid) [PACA] was printable into an object followed by in-situ ultraviolet cross-linking.

With the DIW 3D printing and post-crosslinking, the 3D printed object exhibited vivid structural colors with an angle-independent property. As a result of the synergistic thermally responsive property of PACA and HPC, the resulting 3D printed object also exhibited color tunability under the environmental temperature control, as shown in Fig. 6 (Zhang *et al.* 2022). Similarly, DIW 3D printing is used to print flexible photonic hydrogels. This hydrogel system is combined with acrylamide, photo-initiator Irgacure 2959, cross-linker MBA, and laponite as additives to tailor rheology property. The printed hydrogels had chromatic patterns (Cheng *et al.* 2022). Inspired from the core-shell structure of 3D printed liquid metal and polyacrylate composite liquid crystal fibers (Kotikian *et al.* 2021), a wearable, stretchable, and structure color variable strain sensor composited of polybutylene adipate terephthalate (PBAT) encapsulated HPC-CNT composites was manufactured *via* DIW 3D printing and post-curing treatment. PBAT as a biodegradable

and cheap material was explored as encapsulation to retain the structural colors of HPC, and the purpose of CNT was to impart the printed composite materials with robust electrical conductivity and enhanced color saturation (Wei *et al.* 2022).

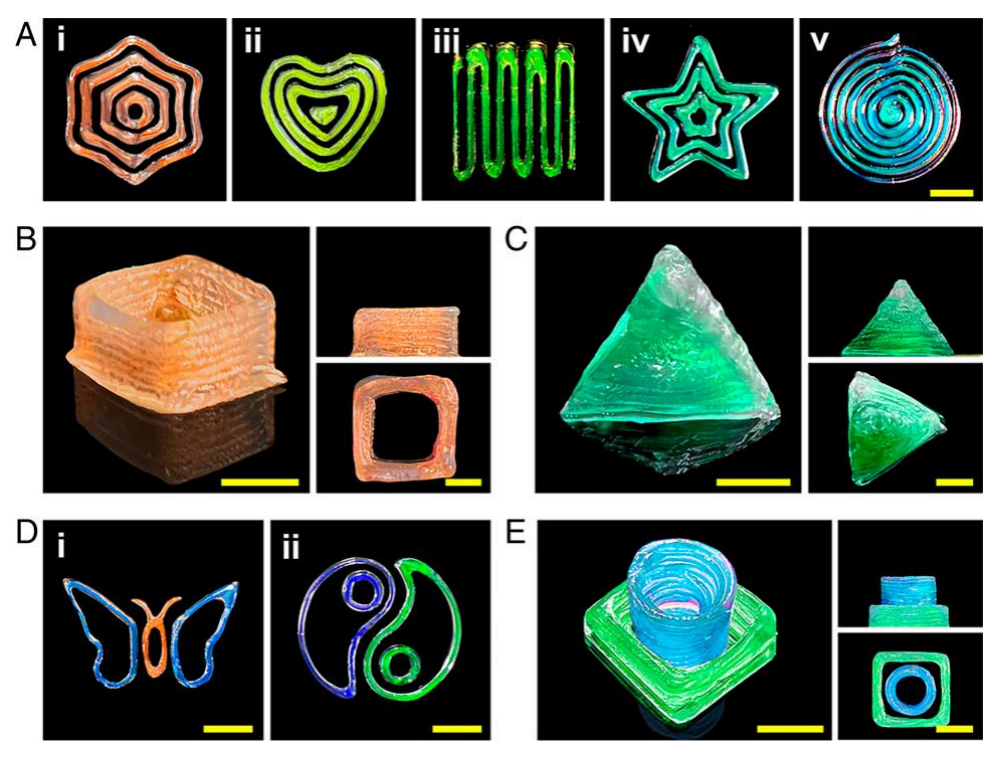


**Fig. 6.** Direct ink writing 3D printing HPC structural color materials (Zhang *et al.* 2022). Figure republished under https://creativecommons.org/licenses/by-nc-nd/4.0/

### **Wet-Spinning HPC or CNC Photonic Materials**

In addition to 3D printing, wet-spinning technology is another way to manufacture fiber materials. As mechanochromic photonic fibers have unique merits, such as fast and efficient color display and visualization, photonic fibers have attracted attention recently. For instance, a color changeable thermochromatic fiber manufacturing method *via* the wet-spinning technique was studied, and these fibers displayed temperature-dependent structural color variations due to the encapsulating thermochromic microcapsules (Li *et al.* 2022). However, the mechanochromic photonic fibers based on synthetic pigments are not environmentally friendly. Therefore, the development of electro- or wet-spinning HPC or CNC liquid crystal photonic fibers with mechano- or thermo-chromic property is an emerging field as the pigment or dye free- CNC or HPC photonic fibers have unique merits, such as biodegradability and freedom from chemical toxicity (Williams *et al.* 2023). For instance, the color tunable CNC photonic fibers composed of CNC as a photonic matrix and PVA as a photonic property modifier was manufactured *via* the wet-spinning technique (Meng *et al.* 2018).

#### CONCLUSIONS AND FUTURE PROSPECTS

The structure and phase transition behavior of chiral liquid crystal HPC solutions and CNC suspensions have been systemically reviewed in this article. The HPC phase diagram involves four phase regimes, while the CNC phase diagram is relatively simple, by contrast. The HPC phase diagram depends on both concentration and temperature. In addition, different characterization tools to evaluate the size, chirality, orientation, and order of liquid crystal HPC and CNC were further explored. Besides, diverse HPC and CNC liquid crystal photonic elastomers were systemically summarized. These elastomer materials involve hydrogel, ionic conductive poly(deep eutectic solvents), conventional rubbery elastomer, and recycled vitrimer with dynamic covalent crosslinking. Finally, different manufacturing techniques including 3D printing, wet-spinning, spray coating, and conventional processing to produce soft matter photonic materials were critically commented on, and these soft matter photonic materials have potential in applications of high-performance and functional photonic fibers, smart coatings, and intelligent packaging (Ehman *et al.* 2023; Triantafillopoulos and Koukoulas 2020).

It is interesting to explore how the combined opposite chirality of HPC and CNC or chitin can affect the photonic elastomer performance, such as HPC and CNC (Walters *et al.* 2020) or chitin and HPC. Due to its unique property of vitrimer in terms of welding, self-healing, shape memory, and recycling, the development of chemically recycling elastomer vitrimer with dynamic covalent network structure requires further study. However, the research in terms of HPC or CNC photonic liquid crystal elastomer vitrimer is in its infancy.

#### **ACKNOWLEDGMENTS**

The Financial support for this work was from the Natural Science Foundation of Hebei Province (Grant No. E2020203063) and Department of Education Foundation of Hebei Province (Grant No. QN2020104).

#### REFERENCES CITED

- Ayrilmis, N. (2020). "Surface properties of oriented strand board coated by electrostatic dry powder spray deposition technique," *BioResources* 15(1), 1521-1530. DOI: 10.15376/biores.15.1.1521-1530
- Atkins, P., and de Paula, J. (2010). *Physical Chemistry*, 9<sup>th</sup> Edition, New York, United States.
- Babaei-Ghazvini, A., and Acharya, B. (2023). "Mechanical responsive visible structural colors based on chiral-nematic cellulose nanocrystals photonic hydrogels," *Chemical Engineering Journal* 476, article 146585. DOI: 10.1016/j.cej.2023.146585
- Bading, M., Olsson, O., and Kümmerer, K. (2024). "Analysis of environmental biodegradability of cellulose-based pharmaceutical excipients in aqueous media," *Chemosphere* 352, article 141298. DOI: 10.1016/j.chemosphere.2024.141298
- Bai, L, Jin, Y., Shang, X., Jin, H. Y., Zhou Y. T., and Shi, L. J. (2021). "Highly synergistic, electromechanical and mechanochromic dual-sensing ionic skin with multiple monitoring, antibacterial, self-healing, and anti-freezing functions," *Journal*

- of Materials Chemistry A 9, 23916-23928. DOI: 10.1039/D1TA06798B
- Boott, C. E., Shi, L., Li, Z. Z., Hamad, W. Y., and MacLachlan, M. J. (2023). "A facile photoinitiated polymerisation route for the preparation of photonic elastomers with chiral nematic order," *Liquid Crystals* 50, 1143-1150. DOI: 10.1080/02678292.2023.2200265
- Boott, C. E., Tran, A., Hamad, W. Y., and MacLachlan, M. J. (2020). "Cellulose nanocrystal elastomers with reversible visible color," *Angewandte Chemie International Edition* 132, 232-237. DOI: 10.1002/ange.201911468
- Boott, C. E., Soto, M. A., Hamad, W. Y., and MacLachlan, M. J. (2021). "Shape-memory photonic thermoplastics from cellulose nanocrystals," *Advanced Functional Materials* 31, 2103268. DOI: 10.1002/adfm.202103268
- Browne, C, Raghuwanshi, V. S., Lin, M. Q., Garnier, G., and Batchelor, W. (2022). "Characterisation of cellulose nanocrystals by rheology and small angle X-ray scattering (SAXS)," *Colloids and Surfaces A: Physicochemical and Engineering Aspects* 651, article 129532. DOI: 10.1016/j.colsurfa.2022.129532
- Bruckner, J. R., Kuhnhold, A., Honorato-Rios, C., Schilling, T., and Lagerwall, J. P. F. (2016). "Enhancing self-assembly in cellulose nanocrystal suspensions using high-permittivity solvents," *Langmuir* 32, 9854-9862. DOI: 10.1021/acs.langmuir.6b02647
- Casay, G. A., George, A., Hadjichristidis, N., Lindner, J. S., Mays, J. W., Peiffer, D. G., and Wilson, W. W. (1995). "Dilute solution properties, chain stiffness, and liquid crystalline properties of cellulose propionate," *Journal of Polymer Science: Part B: Polymer Physics* 33, 1537-1544. DOI: 10.1002/polb.1995.090331011
- Chan, C. L. C., Bay, M. M., Jacucci, G., Vadrucci, R., Williams, C. A., van de Kerkhof, G. T., Parker, R. M., Vynck, K., Frka-Petesic, B., and Vignolini, S. (2019). "Visual appearance of chiral nematic cellulose-based photonic films: angular and polarization independent color response with a twist," *Advanced Materials* 31, article 1905151. DOI: 10.1002/adma.201905151
- Chen, G. J., and Hong, W. (2020). "Mechanochromism of structural-colored materials," *Advanced Optical Materials* 8, article 2000984. DOI: 10.1002/adom.202000984
- Chen, J. S., Zhu, Z. L., Chen, J. Q., Luo, Y. T., Li, L., Liu, K., Ding, S., Li, H., Liu, M. X., Zhou, C. R., and Luo, B. H. (2023). "Photocurable liquid crystal hydrogels with different chargeability and tunable viscoelasticity based on chitin whiskers," *Carbohydrate Polymers* 301, article 120299. DOI: 10.1016/j.carbpol.2022.120299
- Cheng, Q. Y., Guo, J. H., Cao, H. D., and Chang, C. Y. (2022). "The digital printing of chromatic pattern with a single cellulose nanocrystal ink," *Chemical Engineering Journal* 439, article 135670. DOI: 10.1016/j.cej.2022.135670
- Cheung, C. C. Y., Giese, M., Kelly, J. A., Hamad, W. Y., and MacLachlan, M. J. (2013). "Iridescent chiral nematic cellulose nanocrystal/polymer composites assembled in organic solvents," *ACS Macro Letters* 2, 1016-1020. DOI: 10.1021/mz400464d
- Conio, G., Bianchi, E., Ciferri, A., Tealdi, A., and Aden, M. A. (1983). "Mesophase formation and chain rigidity in cellulose and derivatives. 1. (hydroxypropyl)cellulose in dimethylacetamide," *Macromolecules* 16, 1264-1270. DOI: 10.1021/ma00146a012
- Cowie, J. M. G., and Arrighi, V. (2007). *Polymers: Chemistry and Physics of Modern Materials*, 3<sup>rd</sup> Edition, Boca Raton, United States.
- Cui, Q. K., Huang, X., Dong, X. Y., Zhao, H. Y., Liu, X. H., and Zhang, X. X. (2022). "Self-healing bimodal sensors based on bioderived polymerizable deep eutectic solvent ionic elastomers," *Chemistry of Materials* 34, 10778-10788. DOI: 10.1021/acs.chemmater.2c03105

- Dong, X., Wang, Z. L., Song, F., Wang, X. L., and Wang, Y. Z. (2023). "Construction of cellulose structural-color pigments with tunable colors and iridescence/non-iridescence," *Carbohydrate Polymers* 313, article 120877. DOI: 10.1016/j.carbpol.2023.120877
- Droguet, B. E., Liang, H. L., Frka-Petesic, B., Parker, R. M., De Volder, M. F. L., Baumberg, J. J., and Vignolini, S. (2022). "Large-scale fabrication of structurally coloured cellulose nanocrystal films and effect pigments," *Nature Materials* 21, 352-358. DOI: 10.1038/s41563-021-01135-8
- Ebers, L. S., and Laborie, M. P. (2020). "Direct ink writing of fully bio-based liquid crystalline lignin/hydroxypropyl cellulose aqueous inks: Optimization of formulations and printing parameters," *ACS Applied Bio Materials* 3, 6897-6907. DOI: 10.1021/acsabm.0c00800
- Ehman, N., Ponce de León, A., and Area, M. C. (2023). "Fractionation stream components of wood-based biorefinery: New agents in active or intelligent primary food packaging?," *BioResources* 18, 6724-6726. DOI: 10.15376/biores.18.4.6724-6726
- Erdal, N. B., and Hakkarainen, M. (2022). "Degradation of cellulose derivatives in laboratory, man-made, and natural environments," *Biomacromolecules* 23, 2713-2729. DOI: 10.1021/acs.biomac.2c00336
- Espinha, A., Guidetti, G., Serrano, M. C., Frka-Petesic, B., Dumanli, A. G., Hamad, W. Y., Blanco, A., López, C., and Vignolini, S. (2016). "Shape memory cellulose-based photonic reflectors," *ACS Appl. Mater. Interfaces* 8, 31935-31940. DOI: 10.1021/acsami.6b10611
- Fei, Z. X., Lan, J., Sun, J. R., Yin, C. X., and Shi, L. Y. (2023). "Flexible ionic conductors based on polymerized deep eutectic solvent reinforced by hydroxyethyl cellulose," *Polymer* 284, article 126304. DOI: 10.1016/j.polymer.2023.126304
- Fortin, S., and Charlet, G. (1989). "Phase diagram of aqueous solutions of (hydroxypropyl)cellulose," *Macromolecules* 22, 2286-2292. DOI: 10.1021/ma00117a023
- Frank, B. P., Smith, C., Caudill, E. R., Lankone, R. S., Carlin, K., Benware, S., Pedersen, J. A., and Fairbrother, D. H. (2021). "Biodegradation of functionalized nanocellulose," *Environmental Science & Technology* 55, 10744-10757. DOI: 10.1021/acs.est.0c07253
- Gao, J., Haidar, G., Lu, X. H., and Hu, Z. B. (2001). "Self-association of hydroxypropylcellulose in water," *Macromolecules* 34, 2242-2247. DOI: doi.org/10.1021/ma001631g
- George, K., Esmaeili, M., Wang, J. Y., Taheri-Qazvini, N., Abbaspourrad, A., and Sadati, M. (2023). "3D printing of responsive chiral photonic nanostructures," *The Proceedings of the National Academy of Sciences*, 120, article e2220032120. DOI: 10.1073/pnas.2220032120
- Godinho, D. M., Gray, H. G., and Pieranski, P. (2017). "Revisiting (hydroxypropyl) cellulose (HPC)/water liquid crystalline system," *Liquid Crystals* 44, 2108-2120. DOI: 10.1080/02678292.2017.1325018
- Gong, J. P., Katsuyama, Y., Kurokawa, T., and Osada, Y. (2003). "Double-network hydrogels with extremely high mechanical strength," *Advanced Materials* 15, 1155-1158. DOI: 10.1002/adma.200304907
- Guido, S. (1995). "Phase behavior of aqueous solutions of hydroxypropylcellulose," *Macromolecules* 28, 4530-4539. DOI: 10.1021/ma00117a023

- Haywood, A. D., Weigandt, K. M., Saha, P., Noor, M., Green, M. J., and Davis, V. A. (2017). "New insights into the flow and microstructural relaxation behavior of biphasic cellulose nanocrystal dispersions from RheoSANS," Soft Matter 13, 8451-8462. DOI: 10.1039/C7SM00685C
- He, P. S. (2020). Structure and Properties of Polymers, Beijing, China.
- Hiemenz, P. C., and Lodge, T. P. (2007). Polymer Chemistry, 2<sup>nd</sup> Edition, Boca Raton, United States.
- Hubbe, M. A., Tayeb, P., Joyce, M., Tyagi, P., Kehoe, M., Dimic-Misic, K., and Pal, L. (2017). "Rheology of nanocellulose-rich aqueous suspensions: A Review," BioResources 12(4), 9556-9661. DOI: 10.15376/biores.12.4.Hubbe
- Isik, M., Ruiperez, F., Sardon, H., Gonzalez, A., Zulfigar, S., and Mecerreyes, D. (2016). "Innovative poly(ionic liquid)s by the polymerization of deep eutectic monomers," Macromolecular Rapid Communications 37, 1135-1142. DOI: 10.1002/marc.201600026
- Kádár, R., Spirk, S, and Nypelö, T. (2021). "Cellulose anocrystal liquid crystal phases: progress and challenges in characterization sing rheology coupled to optics, scattering, and spectroscopy," ACS Nano 15, 7931-7945. DOI: 10.1021/acsnano.0c09829
- Ko, H., Kim, M., Wi, Y., Rim, M., Lim, S. I., Koo, J., Kang, D. G., and Jeong, K. U. (2021). "Chiroptical smart paints: polymerization of helical structures in cholesteric liquid crystal films," Journal of Chemical Education 98, 2649-2654. DOI: 10.1021/acs.jchemed.1c00168
- Kose, O., Boott, C. E., Hamad, W. Y., and MacLachlan, M. J. (2019). "Stimuliresponsive anisotropic materials based on unidirectional organization of cellulose nanocrystals in an elastomer," *Macromolecules* 52, 5317-5324. DOI: 10.1021/acs.macromol.9b00863
- Kotikian, A., Morales, J. M., Lu, A., Mueller, J., Davidson, Z. S., Boley, J. M., and Lewis, J. A. (2021). "Innervated, self-sensing liquid crystal elastomer actuators with closed loop control," Advanced Materials 33, article 2101814. DOI: 10.1002/adma.202101814
- Kulichikhin, V. G., Makarova, V. V., Tolstykh, M. Y., Picken, S. J., and Mendes, E. (2011). "Structural evolution of liquid-crystalline solutions of hydroxypropyl cellulose and hydroxypropyl cellulose-based nanocomposites during flow," *Polymer* Science Series A 53, 748-74. DOI: 10.1134/S0965545X11090070
- Li, P., Sun, Z. H., Wang, R., Gong, Y. C., Zhou, Y. T., Wang, Y. W., Liu, X. J., Zhou, X. J., Ouyang, J., Chen, M. Z.M., Hou, C., Chen, M., and Tao, G. M. (2022). "Flexible thermochromic fabrics enabling dynamic colored display," Frontiers of Optoelectronics. DOI: 10.1007/s12200-022-00042-3
- Li, X. K., Liu, J. Z., and Zhang, X. X. (2023). "Pressure/temperature dual-responsive cellulose nanocrystal hydrogels for on-demand schemochrome patterning," Advanced Functional Materials 55, article 2306208. DOI: 10.1002/adfm.202306208
- Lu, C. W., Wang, X. Y., Shen, Y., Wang, C. P., Wang, J. F., Yong, Q., and Chu, F. X. (2022). "Liquid-free, anti-freezing, solvent-resistant, cellulose-derived ionic conductive elastomer for stretchable wearable electronics and triboelectric nanogenerators," Advanced Functional Materials 32, article 2207714. DOI: 10.1002/adfm.202207714
- Marchessault, R. H., Morehead, F. F., and Walter, N. M. (1959). "Liquid crystal systems from fibrillar polysaccharides," Nature 184, 632-633. DOI: 10.1038/184632a0

- McCrum, N. G., Buckley, C. P., and Bucknall, C. B. (1997). *Principles of Polymer Engineering*, 2<sup>nd</sup> Edition, New York, United States.
- Meng, X., Pan, H., Lu, T., Chen, Z. X., Chen, Y. R., Zhang, D., and Zhu, S. M. (2018). "Photonic-structured fibers assembled from cellulose nanocrystals with tunable polarized selective reflection," *Nanotechnology* 29, article 325604. DOI: 10.1088/1361-6528/aac44b
- Momen, A., Walters, C. M., Xu, Y. T., Hamad, W. Y., and MacLachlan, M. J. (2021). "Concentric chiral nematic polymeric fibers from cellulose nanocrystals," *Nanoscale Advances* 3, 5111-5121. DOI: 10.1039/D1NA00425E
- Odian, G. (2007). *Principles of Polymerization*, 4<sup>th</sup> Edition, New Jersey, United States. Pan, J. H., Hamad, W., and Straus, S. K. (2010). "Parameters affecting the chiral nematic phase of nanocrystalline cellulose films," *Macromolecules* 43, 3851-3858. DOI: 10.1021/ma902383k
- Peng, N., Huang, D., Gong, C., Wang, Y. X., Zhou, J. P., and Chang, C. Y. (2020). "Controlled arrangement of nanocellulose in polymeric matrix: From reinforcement to functionality," *ACS Nano* 14, 16169-16179. DOI: 10.1021/acsnano.0c08906
- Pignon, F., Challamel, M, Geyer, A. D., Elchamaa, M., Semeraroa, E. F., Hengl, N., Jean, B., Putaux, J. L., Gicquel, E., Bras, J., Prevost, P., Sztuckid, M., Narayanan, T., and Djeridi, H. (2021). "Breakdown and buildup mechanisms of cellulose nanocrystal suspensions under shear and upon relaxation probed by SAXS and SALS," *Carbohydrate Polymers* 260, article 117751. DOI: 10.1016/j.carbpol.2021.117751
- Qu, D., Chu, G., Martin, P., Vasilyev, G., Vilensky, R., and Zussman, E. (2019). "Modulating the structural orientation of nanocellulose composites through mechanostimuli," *ACS Applied Materials Interfaces* 11, 40443-40450. DOI: 10.1021/acsami.9b12106
- Revol, J. F., Bradford, H., Giasson, J., Marchessault, R. H., and Gray, D. G. (1992). "Helicoidal self-ordering of cellulose microfibrils in aqueous suspension," *International Journal of Biological Macromolecules* 14, 170-172. DOI: 10.1016/S0141-8130(05)80008-X
- Roe, R. J. (2000). *Methods of X-ray and Neutron Scattering in Polymer Science*, 1<sup>st</sup> Edition, Oxford, England.
- Rubinstein, M., and Colby, R. H. (2003). Polymer Physics, Oxford, England.
- Shi, H. D., Deng, Y. X., and Shi, Y. (2023). "Cellulose-based stimuli-responsive anisotropic hydrogel for sensor application," *ACS Applied Nano Materials* 6, 11524-11530. DOI: 10.1021/acsanm.3c01551
- Singh, S., Bhardwaj, S., Verma, C, Chhajed, M, Balayan, K., Ghosh, K., and Maji, P. K. (2022). "Elliptically birefringent chemically tuned liquid crystalline nanocellulose composites for photonic applications," *Journal of Molecular Liquids* 366, article 120326. DOI: 10.1016/j.molliq.2022.120326
- Solomons, T. W. G., and Fryhle, C. B. (2011). *Organic Chemistry*, 10<sup>th</sup> Edition, Hoboken, United States.
- Sui, Y. Q., Li, X. F., Chang, W., Wan, H., Li, W., Yang, F., and Yu, Z. Z. (2020). "Multi-responsive nanocomposite membranes of cellulose nanocrystals and poly(N-isopropyl acrylamide) with tunable chiral nematic structures," *Carbohydrate Polymers* 232, article 115778. DOI: 10.1016/j.carbpol.2019.115778
- Sun, S. F. (2004). *Physical Chemistry of Macromolecules: Basic Principles and Issues*, New York, United States.
- Sun, J. Y., Zhao, X. H., Widusha R. K., Chaudhuri, I. O., Oh, K. H., Mooney, D. J.,

- Vlassak, J., and Suo, Z. J. (2012). "Highly stretchable and tough hydrogels," *Nature* 489, 133-136. DOI: 10.1038/nature11409
- Triantafillopoulos, N., and Koukoulas, A. A. (2020). "The future of single-use paper coffee cups: Current progress and outlook," *BioResources* 15(3), 7260-7287. DOI: 10.15376/biores.15.3.Triantafillopoulos
- Vogler-Neuling, V. V., Saba, M., Gunkel, I., Zoppe, J. O., Steiner, U., Wilts, B. D., and Dodero, A. (2023). "Biopolymer photonics: From nature to nanotechnology," *Advanced Functional Materials* 2306528. DOI: 10.1002/adfm.202306528
- Vollick, B., Kuo, P. Y., Thérien-Aubi, H., Yan, N., and Kumacheva, E. (2017). "Composite cholesteric nanocellulose films with enhanced mechanical properties," *Chemistry of Materials* 29, 789-795. DOI: 10.1021/acs.chemmater.6b04780
- Vshivkov, S. A., and Rusinova, E. V. (2007). "Phase diagrams of a hydroxypropyl cellulose-water system under static conditions and in the shear field," *Polymer Science Series B* 49, 209-212. DOI: 10.1134/S1560090407070093
- Wang, J. M., Cheng, Q. Y., Feng, S. Y., Zhang, L. N., and Chang, C. Y. (2021). "Shear-aligned tunicate-cellulose-nanocrystal-reinforced hydrogels with mechano-thermochromic properties," *Journal of Materials Chemistry* 9, 6344-6350. DOI: 10.1039/D1TC00911G
- Wang, C., Lin, X., Schäfer, C. G., Hirsemann, S., and Ge, J. P. (2021). "Spray synthesis of photonic crystal based automotive coatings with bright and angular-dependent structural colors," *Advanced Functional Materials* 31, article 2008601. DOI: 10.1002/adfm.202008601
- Wang, P., Qian, X., and Shen, J. (2018). "Superhydrophobic coatings with edible biowaxes for reducing or eliminating liquid residues of foods and drinks in containers," *BioResources* 13(1), 1-2.
- Walters, C. M., Boott, C. E., Nguyen, T. D., Hamad, W. Y., and MacLachlan, M. J. (2020). "Iridescent cellulose nanocrystal films modified with hydroxypropyl cellulose," *Biomacromolecules* 21, 1295-1302. DOI: 10.1021/acs.biomac.0c00056
- Wei, J. J., Aeby, X., and Nyström, G. (2022). "Printed structurally colored cellulose sensors and displays," *Advanced Materials Technologies* 8, article 2200897. DOI: 10.1002/admt.202200897
- Weißenborn, E., and Braunschweig, B. (2019). "Hydroxypropyl cellulose as a green polymer for thermo-responsive aqueous foams," *Soft Matter* 15, 2876-2883. DOI: 10.1039/C9SM00093C
- Werbowyj, R. S., and Gray D. G. (1980). "Ordered phase formation in concentrated hydroxypropylcellulose solutions," *Macromolecules* 13, 69-73. DOI: 10.1021/ma60073a014
- Werbowyj, R. S., and Gray, D. G. (1984). "Optical properties of (hydroxypropyl) cellulose liquid crystals. cholesteric pitch and polymer concentration," *Macromolecules* 17, 1512-1520. DOI: 10.1021/ma00138a016
- Werbowyj, R. S., and Gray, D. G. (1976). "Liquid crystalline structure in aqueous hydroxypropyl cellulose solutions," *Molecular Crystals and Liquid Crystals* 34, 97-103. DOI: 10.1080/15421407608083894
- Williams, M. W., Wimberly, J. A., Stwodah, R. M., Nguyen, J., D'Angelo, P. A., and Tang, C. (2023). "Temperature-responsive structurally colored fibers *via* blend electrospinning," *ACS Applied Polymer Materials* 5, 3065-3078. DOI: 10.1021/acsapm.3c00222

- Winnik, F. M., Winnik, M. A., and Tazuke, S. (1987). "Synthesis and characterization of pyrene-labeled (hydroxypropyl) cellulose and its fluorescence in solution," *Macromolecules* 20, 38-44. DOI: 10.1021/ma00167a008
- Xie, M., Chen, J., Zhang, T., and Sun, X. (2023). "Angle-independent cellulosic photonic crystals for smart and sustainable colorimetric sensing," *BioResources* 18(4), 6731-6733. DOI: 10.15376/biores.18.4.6731-6733
- Xue, R., Zhao, H., An, Z. W., Wu, W., Jiang, Y., Li, P., Huang, C. X., Shi, D., Li, R. K. Y., Hu, G. H., and Wang, S. F. (2023). "Self-healable, solvent response cellulose nanocrystal/waterborne polyurethane nanocomposites with encryption capability," ACS Nano 17, 5653-5662. DOI: 10.1021/acsnano.2c11809
- Yi, H., Lee, S. H., Ko, H., Lee, D., Bae, W. G., Kim, T., Hwang, D. S., and Jeong, H. E. (2019). "Ultra-adaptable and wearable photonic skin based on a shape-memory, responsive cellulose derivative," *Advanced Functional Materials* 29, article 1902720. DOI: 10.1002/adfm.201902720
- Zhang, J. L., Wu, Q. L., Li, M. C., Song, K. L., Sun, X. X., Lee, S. Y., Lei, T. Z. (2017). "Thermoresponsive copolymer poly(N-vinylcaprolactam) grafted cellulose nanocrystals: Synthesis, structure, and properties," *ACS Sustainable Chemistry & Engineering* 5, 7439-7447. DOI: 10.1021/acssuschemeng.7b02033
- Zhang, Z. L., Dong, X., Fan, Y. N., Yang, L. M., He, L., Song, F., Wang, X. L., and Wang, Y. Z. (2020). "Chameleon-inspired variable coloration enabled by a highly flexible photonic cellulose film," *ACS Applied Materials & Interfaces* 12, 46710-46718. DOI: 10.1021/acsami.0c13551
- Zhang, Z. H., Chen, Z. Y., Wang, Y., and Zha, Y. J. (2020). "Bioinspired conductive cellulose liquid-crystal hydrogels as multifunctional electrical skins," *Proceedings of the National Academy of Sciences* 117, 18310-18316. DOI: 10.1073/pnas.200703211
- Zhang, Z. H., Chen, Z. Y., Shang, L. R., and Zhao, Y. J. (2021). "Structural color materials from natural polymers," *Advanced Materials Technologies* 6, article 2100296. DOI: 10.1002/admt.202100296
- Zhang, Z. H., Wang, C., Wang, Q., and Shang, L. R. (2022). "Cholesteric cellulose liquid crystal ink for three-dimensional structural coloration," *The Proceedings of the National Academy of Sciences* 119, article e2204113119. DOI: 10.1073/pnas.2204113119
- Zhang, J. L., Li, W. G., and Wu, Q. L. (2023). "Design of chemically recyclable nanocellulose chiral liquid crystal photonic elastomer vitrimer and its mechanosensitive colour-changing materials," *BioResources* 18(4), 6727-6730. DOI: 10.15376/biores.18.4.6727-6730

Article submitted: March 13, 2024; Peer review completed: March 30, 2024; Revised version received: April 3, 2024; Accepted: April 4, 2024; Published: October 8, 2024. DOI: 10.15376/biores.19.4.Zhang3